Quantum size effects in equilibrium lithium ultrathin layers

J. C. Boettger
Theoretical Division, Los Alamos National Laboratory, Los Alamos, New Mexico 87545

S. B. Trickey*
Center for Materials Science, Los Alamos National Laboratory, Los Alamos, New Mexico 87545
(Received 10 May 1991)

The existence and extent of quantum size effects in simple metal ultrathin films are studied by a systematic local-density, all-electron, full-potential calculation of the cohesive properties of ν layers of hexagonal Li, with $\nu=1$, 2, 3, 4, and 5. By $\nu=5$, there is clear convergence of the a lattice parameter (intraplanar bond length) to very nearly the calculated crystalline value, with a distinction between the two films with a meaningful interior ($a=5.68\pm0.01$ a.u. for $\nu=4$ and 5) and those with a minimal interior or none at all ($\nu=3$ and $\nu=1$ and 2, respectively; $a=5.75^{+0.02}_{-0.01}$ a.u.). Equally clear stability of the interplanar spacings occurs at distinctly *noncrystalline* values (4.27 a.u. for $\nu=2$; 4.38 ± 0.01 a.u. for the inner spacing of $\nu=3$, 4, and 5 versus 4.64 a.u. for the crystalline calculation). The cohesive energies of the 3, 4, and 5 layers are closely clumped at about 87% of the crystalline value. As the 2 and 1 layers are substantially less bound, both the cohesive properties and the inner interplanar spacing suggest a different grouping than suggested by the a lattice parameter. Rough extrapolation of the slowly increasing cohesion with ν suggests that $\nu\approx20$ would be needed to achieve even 90% of the crystalline cohesive energy. The calculated surface energies do not exhibit any strong size effect, in striking contrast to Al films. The equilibrium intraplanar force constant a^2E/da^2 has a minimum at $\nu=3$, with its maximum at $\nu=5$ almost 2.5 times larger. The calculated work functions give only a hint, at the very most, of the quantum size oscillations predicted from jellium models. A significant quantum size effect occurs, however, in the occupied portion of the density of states, which exhibits a step-function increase for each integer increase in ν. The density of states at E_F has a maximum at $\nu=3$ with a variation over the series of about 10%. The unrelaxed films do not exhibit a stronger quantum size effect than the equilibrium films, again with the barely possible exception of the work function.

I. BACKGROUND, MOTIVATION

Ever since the prediction of thickness-dependent oscillations in the work function of an extremely thin jellium film,[1,2] there have been open questions about the existence of such static quantum size effects (QSE) in ultrathin films of real metals and about the magnitude of QSE if they exist. The underlying issue is the much-documented dependence of one-electron properties upon lattice structure and spacings: will a real ultrathin system reconstruct relative to its crystalline counterpart in a way which suppresses otherwise expectable QSE? The relatively small number of studies on the subject[3–8] suggest that structural changes with the number of layers tend to reduce but not eliminate QSE. However, the evidence is hardly conclusive.

Part of the problem is that theoretical prediction of the equilibrium structural properties of ultrathin films (ν-layers with $\nu=1,2,3,\ldots$ atomic layers) is considerably more demanding than treatment of their electronic properties with the structure corresponding to a fixed slice from the parent crystal. Thus, the most extensive investigations of possible QSE in a sequence of real films are for Al in unrelaxed (so-called ideal) system geometries (Feibelman and Hamann[4] and Batra *et al.*[7]). In the case of Ref. 7 only films with an odd number of layers were treated. Both calculations found large (≈0.6–1.1 eV) work-function variations with layer number. Apparently the real systems most commonly thought of as well modeled by jellium treatments, the alkali metals, have never been examined for QSE.

Structural optimization studies to date (especially those using all-electron methodologies) seem to be concentrated either on 1 and 2 layers (see Ref. 9 for references) or upon the modeling of relaxation at solid surfaces by treatment of thicker films with inversion symmetry ($\nu=2s+1$, with typically $s=3,\ldots,7$). To our knowledge no systematic prediction of the structural equilibria and properties of an uninterrupted sequence of ultrathin films with $\nu>2$ has ever appeared. It appears that the only structural equilibrium calculations on 1- and 2-L pairs reported to date are Feibelman's for Al,[3] ours for Be,[10–12] H (Wu *et al.*[13]), Li (Boettger *et al.*[9]), and a preliminary study of graphite (Trickey, Diercksen, and Müller-Plathe[14]). Even those exhibit somewhat counter-intuitive results.

The unusual nature of the trends in ν-layer structural parameters, relative to crystalline values, was discussed in detail in Ref. 9 so a summary suffices. Simple coordination number arguments (in the absence of symmetry-changing reconstructions and with due consideration of the number of neighboring layers, if any) lead to the expectation that an unsupported metallic 1-L should exhibit reduced intraplanar separation relative to the bulk value.

The 2-L should, on the same grounds, have an intraplanar separation intermediate between the 1-L and the crystal, while the asymmetry of 2-L interplanar binding should reduce the 2-L interplanar separation somewhat from the crystalline value. Adding layers should then cause a smooth increase in the intraplanar lattice parameter and a rapid approach to the theoretical crystalline value. Similarly a relatively thick film ought to have an interior interplanar separation essentially identical with the bulk crystal value, with smaller values near the film surfaces.

That picture is the "coordination model" discussed in Ref. 9. As shown there, what actually happens in even the Li 1-L, 2-L pair is rather different. In both, the intraplanar separation is *expanded* relative to the calculated crystalline value (1.6% and 2.8%, for the 1-L and 2-L, respectively). The 2-L interplanar distance is substantially contracted (dilayer $c/a \cong 1.464$ versus calculated bulk $\cong 1.644$). The predicted 1-L and 2-L work functions differed little (3.53 and 3.58 eV, respectively), a somewhat disquieting outcome to anyone with expectations (from the jellium calculations) of work function QSE in Li.

The Li 1-L and 2-L findings were sufficiently intriguing to motivate study of as large a sequence of ν layers of Li as is computationally tractable. Here we report the outcome of that systematic study of the cohesive and one-electron properties of ν layers of Li with $\nu = 1$, 2, 3, 4, and 5. The remaining sections summarize methodology, present the energetics and equilibrium lattice parameters, consider force constants and equations of state, and conclude with electronic structure [at the level of Kohn-Sham (KS) eigenvalues]. Other earlier work by us on the Li 1 L to which these results are related is found in Refs. 15 and 16. The present results are consistent with those studies as well as with the 1-L and 2-L predictions of Boettger *et al.*[9]

II. METHODOLOGY

The well-known Hedin-Lundqvist (HL) form of local-density approximation (LDA) to density-functional theory (DFT) was used throughout (for references to DFT, LDA, etc., see Kryachko and Ludeña,[17] Dreizler and Gross,[18] and Trickey[19]). The LDA is implemented as a completely first-principles methodology (all-electron, full-potential, full self-consistency at every set of lattice parameters) in the FILMS program package.[9,15,16] FILMS is based upon the linear combination of Gaussian-type orbitals, fitting-function (LCGTO-FF) procedure.[20] The essence of those algorithms is to expand the KS orbitals, the electron number density, and the LDA exchange-correlation kernels in three basis sets, respectively, the KS, Q, and XC bases. These are Hermite Gaussian (for ease of integral evaluation) which are then combined to form appropriate Cartesian Gaussians. As experience with the LCGTO-FF technique has grown it has become clear that identical Q and XC bases are preferred. This single-fitting basis is referred to hereafter as the F basis. The same procedure was used in our previous work on the Li 1- and 2-L films.[9]

Orbital exponents and contraction coefficients for basis sets used in this study are given in Table I. Given the importance of basis set selection in any work such as this, a thorough discussion of how the basis sets in Table I were obtained is warranted. First, it should be noted that at the time of the work reported in Ref. 9, a great deal of care was taken to ensure that the basis sets used there were substantially richer than was necessary for that investigation. Several basis sets were tested and the final results for the 1-L were compared with those obtained with previous basis sets (including one numerical basis set calculation; see Ref. 9 for details). In the present work, we have reduced the size of the F basis while taking care

TABLE I. KS- and F-basis set exponents (ζ) and KS-basis contraction coefficients (C). In the columns marked ν, notations are given to indicate the systems (1, 2, 3, 4, and 5 layer) and sites (int., interior; ext., exterior) for which a given basis function is used ("all" means the function was used for all sites in all systems).

KS basis				F basis		
l	ζ	C	ν	l	ζ	ν
s	1359.446 600	0.000 844	all	s	700.00	all
	204.026 470	0.006 485	all		140.00	all
	46.549 541	0.032 466	all		35.00	all
	13.232 594	0.117 376	all		11.00	all
	4.286 148	0.294 333	all		3.60	all
	1.495 542	1.000 000	all		1.20	all
	0.542 238	1.000 000	all		0.45	all
	0.120 000	1.000 000	3–5 (int.)		0.20	3–5 (int.)
	0.073 968	1.000 000	1–5 (ext.)		0.16	1–5 (ext.)
	0.028 095	1.000 000	1–3,5 (ext.)		0.06	1–5 (ext.)
	(0.030 095)	1.000 000	4 (ext.)			
p	1.4880	0.038 770	all	d	0.40	all
	0.2667	0.236 257	all		0.15	1–5 (ext.)
	0.1500	1.000 000	all			
p_z	0.06	1.000 000	1–5 (ext.)	p_z	0.40	2–5 (ext.)
					0.15	2–5 (ext.)

to ensure that the results for the 1 L and 2 L do not differ significantly from those reported in Ref. 9. Hence, the basis sets used here are well tested and of good quality. Now consider each basis set in more detail.

The KS basis was developed by modification of those from standard sources (9s from van Duijneveldt,[21] p basis from Dunning and Hay[22]). The modifications were guided by application of two empirically based rules: (1) functions centered on outer-layer sites should have atomiclike s and p submanifolds (their most diffuse members should be similar to those of an atomic basis); (2) functions centered on interior-layer sites as well as the entire p_{xy} submanifold should be crystallinelike (the more diffuse functions should be relatively compact to avoid approximate linear dependencies). The basis sets were also modified by contracting the tighter s functions using 1s atomic orbital coefficients from van Duijneveldt.[21]

The primary purpose of these guidelines is to adapt the basis sets to the physical differences between interior and exterior sites for the 3, 4, and 5 L's. Table I shows that the distinction is achieved by a few simple choices involving the more diffuse functions. For example, the uncontracted KS basis is $9s3p_{xy}4p_z$ for exterior sites versus $8s3p$ for interior ones. Comparison of Table I with the corresponding table of our 1-L, 2-L study[9] will show that the KS basis used there needed very little change in order to be suited to the present purpose.

The F-basis set was established primarily on the basis of experience with previous calculations. The result is both a simpler and more effective F basis than was used in the prior 1-L, 2-L study. The results presented here show that the new F basis does not alter the predictions of that study in any substantive way. For the s submanifold, the number of functions and the smallest exponent were initially chosen to be roughly the same as for the KS basis. Starting with the next smallest exponent, the set was tempered with the first interval about a factor of 2 and subsequent intervals growing larger as the exponents increase. This procedure is aimed at assuring that the F basis will have its greatest flexibility in the bonding region. After testing, the smaller exponents were increased as needed to ensure that there were no instabilities in the calculations. The F-basis set was also augmented with d-type Gaussians with angular dependence of the form $z^2-\frac{1}{2}(x^2+y^2)$, with exponents selected to produce added flexibility in the bonding region. Similarly, the F basis for exterior sites was augmented with p_z-type Gaussians. Identical F functions residing in layers which are equivalent by symmetry are contracted also.

Two other remarks should be made about fitting basis exponents for films. First, early work using LCGTO-FF methodology used guidelines due to Dunlap, Connolly, and Sabin[23] to generate Q and XC exponents from the KS exponents. Those guidelines follow from approximate relationships among the three bases which hold in an isolated atom. As such, the guidelines are both appealing and useful in atoms and molecules. The behavior of charge densities and energy densities in extended systems, however, is such that we have found it more effective to generate the F basis independent of the details of the KS basis. Thus we no longer use the guidelines of Dunlap, Connolly, and Sabin. Second, in their pioneering study of QSE, Feibelman and Hamann[4] remarked that they had turned away from their implementation of fitting-function methodology because of problems with regions of negative density. With sufficient attention to the F basis and technical details of the fitting procedure, such problems need not occur and do not in this calculation.

Linear triangle Brillouin-zone (BZ) integration was used with a 37-point mesh in the irreducible wedge of the two-dimensional BZ. Details of the spatial distribution of points are in the Appendix of Ref. 9. All calculations were stabilized to an iteration-to-iteration shift in total energy per atom of less than 1 μH (1H=27.2117 eV).

III. EQUILIBRIUM LATTICE PARAMETERS AND STRUCTURAL ENERGETICS

Because uncertainty still exists as to the exact nature of the close packing in the $T=0$ K, $P=0$ phase of crystalline Li (Ref. 24) and because modern LDA calculations of Li phase stability have been restricted to hcp, fcc, and bcc with hcp found to be energetically preferred,[25–27] we assume hcp ordering for the reference crystal. That ordering, the coordination model, and the previous studies of the Li 1 and 2 L's all point at the hexagonal films as the appropriate targets for study.

The intraplanar unit cell parameter (hexagonal bond length) will be denoted as a. The interplanar separations will be designated as s_i, and s_e (where i refers to distance between interior layers and e to distance between an exterior layer and the next one inward) or merely s as appropriate. The nearest-neighbor spacing is denoted a_{NN}.

Study of 1 through 5 layers requires the optimization of multiple geometric parameters within a finite, computationally tractable number of parameter sets, so a careful strategy for selecting those sets is a necessity. In part the selection is related to the functions to be used in fitting the calculated points. Details of both the search grids and fitting functions utilized are given in the Appendix.

The calculated equilibrium lattice parameters are in Table II, along with calculated and measured results for crystalline Li. We have discussed elsewhere[9] the necessity of comparing to calculated crystalline lattice parameters in order to distinguish a legitimate prediction of lattice contraction from the systematic contraction that LDA models show with respect to experimental values.[28–30] Note, for example, the 3–4 % contraction of calculated crystalline lattice constants as compared to the experiment[31] in Table II. Also note that the Dacorogna and Cohen calculation[25] exhibits less contraction for two reasons: the use of a pseudopotential and of a different LDA model. Except where noted we will compare with the all-electron calculation of Nobel *et al.*[27] which used the same LDA.

Certainly the most remarkable qualitative feature revealed by Table II is that even the interior of the 5 L does not come close to reproducing the interplanar lattice spacing of the crystal. Instead, the value of s_i is sensibly constant for $\nu=4$ and 5 (and matches the s for $\nu=3$) at about 5.6% contraction relative to the crystal, with s_i/a also remarkably stable at 0.77, about 6.4% contracted.

TABLE II. Comparison of calculated and measured Li lattice parameters; see text for notation.

System	a (a.u.)	s_i (a.u.)	s_e (a.u.)	a_{NN} (a.u.)
1 L	5.73			5.73
2 L	5.76		4.27	5.41
3 L	5.75		4.39	5.50
4 L	5.69	4.38	4.32	5.43
5 L	5.67	4.37	4.41	5.49
hcp crystal[a]	5.65	4.64	4.64	5.65
hcp crystal[b]	5.77	4.71	4.71	5.77
hcp crystal expt.[c]	5.88	4.81	4.81	5.88
1 L[d]	5.74			5.74
2 L[d]	5.81		4.25	5.41

[a]Reference 27.
[b]Reference 25.
[c]Reference 31.
[d]Reference 9.

The first of several even versus odd ν distinctions is evident in s_e: $s_e(\nu=3,5)=4.40\pm0.01$ a.u. $s_e(\nu=2,4)=4.29^{+0.03}_{-0.02}$ a.u. In confirmation of the previous calculation, the 2 L is contracted in s by 8% with s/a reduced by 9.8%. Also to be noted is that the 5 L exhibits only rather weak surface relaxation, $s_e/s_i=1.01$.

Quite different behavior is displayed by the a parameter. The dual constraints of an a value common to all planes and lattice translational symmetry in those planes apparently drives the a lattice constant to converge to its crystalline value much more rapidly with respect to ν than is the case with s, which is subject to neither requirement. Thus, a for $\nu=1$, 2, and 3 is expanded with respect to the crystal (behavior already found for $\nu=1$ and 2; see Ref. 9). By $\nu=5$, however, a is essentially indistinguishable from the crystalline value. In fact there is a clear segregation of the two films with a meaningful interior ($\nu=4$ and 5) from those with a minimal interior ($\nu=3$) or none at all ($\nu=1$ and 2): $a=5.68\pm0.01$ a.u. for $\nu=4$ and 5 vs $a=5.75^{+0.01}_{-0.02}$ a.u. for $\nu=1$, 2, and 3.

Values of a_{NN} tabulated in Table II again show an even-odd variation; the larger distances are associated with odd values of ν and the smaller distances with even values of ν (the same pattern found in s_e). Setting aside the monolayer value, the separation is as large as in s_e, $a_{NN}(\nu=2,4)\approx5.40$ a.u., $a_{NN}(\nu=3,5)\approx5.50$ a.u. Put another way, all the ν layers beyond the 1 L have *contracted* nearest-neighbor bonds compared to the crystal. This behavior, when coupled with the lattice expansion in a for $\nu=1$, 2, and 3 and the d contraction for $\nu=2$–5, can be related to the assumptions of the coordination model, i.e., that bonds are contracted in low-ν systems. This expectation is realized for all but $\nu=1$ in Li. The 1 L lies so high in energy relative to the 2 L that it is almost surely the constraint to planarity which prevents the 1 L from fitting into this bonding picture as well.

A somewhat different grouping among the five systems is suggested by the cohesive energies E_c tabulated in Table III. [The reference atomic energy is the local spin-density approximation (LSDA) value from the HL LSDA in a corresponding basis: $E_{\rm tot}=-7.353\,739$ H.] For $\nu=3$, 4, and 5, the cohesive energies cluster within 50 meV whereas the 2 L is 90 meV less bound than the 3 L, and the 1 L is another 290 meV less bound. In terms of the crystalline cohesive energy, the 3, 4, and 5 L all cluster around 86–88 % while the 2 L and 1 L achieve only 80% and 64%, respectively.

Table III also presents, parenthetically, the cohesive

TABLE III. Calculated equilibrium-cohesive energies E_c (eV/atom), incremental energies $E_{\rm inc}$ (eV, see text), interplanar binding energies E_i (eV/atom, see text), and the ratio of E_i to its crystalline value $E_i(\infty)$. Parenthetical entries for E_c refer to the film constrained to be at calculated crystalline lattice parameters (so-called ideal geometry).

System	$-E_c$	$E_{\rm inc}$	$-E_i$	$E_i/E_i(\infty)$
1 L	1.10 (1.10)		0.00	0.00
2 L	1.39 (1.38)	1.68	0.29	0.46
3 L	1.48 (1.47)	1.66	0.38	0.60
4 L	1.51 (1.50)	1.60	0.41	0.65
5 L	1.53 (1.52)	1.61	0.43	0.68
Crystal[a]	1.73	1.73	0.63	1.00
1 L[b]	1.09			
2 L[b]	1.38	1.67	0.29	0.46

[a]Reference 27.
[b]Reference 9.

energies for the films constrained to reside at crystalline lattice parameters. Even though the shifts from crystalline to equilibrium lattice parameters are substantial, especially in s_i and s_e, there is no correspondingly large shift in E_c. At least so far as structural energetics are concerned, there is no masking of QSE by relaxation of the films to equilibrium lattice parameters. We will return to this question in the discussion of one-electron energies (below).

Another way to examine convergence toward the crystalline binding is to seek trends in the incremental binding energy

$$E_{\rm inc}(\nu)=|E_{\rm cell}(\nu)-E_{\rm cell}(\nu-1)| \ . \tag{1}$$

In the limit of arbitrary thickness $E_{\rm inc}$ should approach the magnitude of E_c. The values in Table III are distinct from that limit, even allowing for the quite reasonable possibility of precision limits (due to methodology) of ± 0.03 eV/atom for both $E_c(\infty)$ and $E_{\rm inc}(\nu)$. The slow convergence of both E_c and $E_{\rm inc}$ toward the crystalline value is another striking demonstration of the fundamental difference between ν layers, which lack translationally equivalent neighbors to arbitrary distance in the z direction and the crystalline solid, which has such neighbors.

Table III also shows interplanar binding energies E_i calculated as

$$E_i=E_c(\nu)-E_c(1) \ . \tag{2}$$

Because E_i is the energy advantage per layer of the equilibrium ν layer with respect to ν well-separated 1 L's, it provides another focus on the progression toward crystalline binding. Again the 3-, 4-, and 5-L grouping is manifest. An interesting approximate fit to the calculated ratio $R_i(\nu)=E_i(\nu)/E_i(\infty)$ is

$$R_i(\nu)\approx[\arctan[0.12(\nu-1)]/\arctan(\infty)]^{0.29} \ . \tag{3}$$

This expression (rms deviation = 0.014) yields the prediction that progression to as little as 90% of the crystalline interlayer binding could only be achieved by going to $\nu=17$ (95% would require $\nu=33$). This fit and the behavior of E_c, $E_{\rm inc}$, and E_i all demonstrate that a rather thick film (as measured by multiples of interatomic spacing) is required if macroscopic crystal properties are to be recovered.

Batra *et al.*[7] found that the surface energy

$$E_s(\nu)=\tfrac{1}{2}\nu[E_c(\nu)-E_c(\infty)] \tag{4}$$

of unrelaxed Al (111) films with $\nu=1$, 3, 5, and 7 exhibited a moderate QSE in that E_s ranged up and back down by about 12%. The results in Table IV show that such behavior is not evident in the Li films for $\nu=1,\ldots,5$. Instead E_s seems to be increasing with ν. The two calculations are not completely inconsistent, since it is at least conceivable that a dropoff of E_s could occur in the Li films by $\nu=7$. It is noteworthy, though, that in the Li films the first interior layer is worth about 0.04 eV/atom in E_s with successive interior layers gaining 0.06 eV/atom each. If there is a QSE dropoff in E_s for Li analogous with Al, this trend would have to undergo an abrupt reversal.

TABLE IV. Calculated surface energies E_s (eV/atom) as a function of layer number ν for optimized Li films (present work) and for unrelaxed Al films (Ref. 7).

ν	E_s(Li)	E_s(Al)
1	0.32	0.47
2	0.34	
3	0.38	0.50
4	0.44	
5	0.50	0.49
6		
7		0.44

Although E_s does not display an obvious QSE, both the cohesive energies and d values (Tables II and III) can be interpreted as subdividing the ν layers of Li into three groups, $\nu=1$, $\nu=2$, and $\nu=3$, 4, and 5. This interpretation rests on recognition that identification of $s(\nu=2,3)$ as s_i or s_e is not inexorable. Thought of as s_i, there is a structural size effect in the s parameter which distinguishes the $\nu=3$, 4, and 5 systems from both the crystal and the 1 L and 2 L. Evidently it is related to the fact that only $\nu=3$, 4, and 5 have a populated interior. As already noted, when $s(\nu=2,3)$ is grouped with s_e (as in Table II), there is a well-defined oscillatory QSE in s_e. In either case, it is clear that while the $\nu=3$, 4, and 5 systems have settled on the crystalline a parameter, neither their s parameters nor cohesive energies have settled correspondingly.

Both the a lattice parameter and the uniaxial force constants (energy second derivatives evaluated at equilibrium: d^2E/da^2; d^2E/ds_k^2, $k=i,e$) call attention to a different grouping. Results obtained by the fitting procedures described above are presented in Table V. We have not tabulated the mixed partial derivatives, e.g., $d^2E/da\,ds$, since at each ν they are at most about one-fifth of the smallest magnitude uniaxial derivative. That smallness confirms what is observed while doing the calculations: the variation of the total energy with each lattice parameter is only weakly coupled to the other lattice parameters. Table IV shows that there is a qualitative difference between $\nu=1$, 2, and 3 and $\nu=4$ and 5 not only for a but for the force constants as well. As already remarked, a is nearly constant for $\nu=1$, 2, and 3, yet

TABLE V. Calculated uniaxial force constants as a function of ν (eV/a.u.^{2}). The hcp crystal value was obtained by conversion of the uniaxial compressibility given by Ref. 25.

ν	d^2E/da^2	d^2E/ds_i^2	d^2E/ds_e^2
1	0.40		
2	0.35		0.15
3	0.23		0.14
4	0.33	0.06	0.11
5	0.55	0.10	0.14
hcp		0.30	

d^2E/da^2 drops steadily with ν. That drop appears to be due to improved screening of the intraplanar neighbors by the p_z states of adjacent layers. Detailed examination of the numerical results suggests that the 3 L may even be softer in the a direction than the value of d^2E/da^2 would suggest. For $a=5.70$, 5.75, and 5.80 a.u., the energy minimum as a function of d is nearly a constant. Thus atoms are nearly free to move over that range of a values and, at $\nu=4$, the intraplanar spacing collapses to what is nearly the bulk crystalline value. At the same thickness d^2E/da^2 jumps back up almost to its $\nu=2$ value and rises to 0.55 eV/a.u.^{2} at $\nu=5$, a very substantial value when compared, for example, with the uniaxial crystalline force constant for the s direction.

Elsewhere we have considered[9,16] the scale length L_i for the interplanar energy, which appears in the empirically discerned universal equation of state.[32,33] For the 2 L, L_i is given unambiguously by

$$L_i=[|2E_i|/(d^2E_c/ds^2|_{\min})]^{1.2} \tag{5}$$

with the factor of 2 in the numerator to accord with the definition of L_s, the surface-surface scaling length, used by Ref. 32.

It is less straightforward to define a suitably generalized interlayer energy for the ν layers nor is the proper choice of force constant completely obvious. If however the focus is on thickness changes due to displacements of the two outermost layers, then a plausible choice for the relevant delamination energy (which reduces to the previously used value for $\nu=2$) is

$$E_d=[\nu/(2-\delta_{\nu,2})][E_c(\nu)-(1-2/\nu)E_c(\nu-2) -(2/\nu)E_c(1)] . \tag{6}$$

The numerator of the first factor accounts for what would otherwise be the vanishingly small 1 L contribution for thick systems while the denominator takes care of the difference between the number of exterior thicknesses for $\nu=2$ and $\nu>2$. The appropriate derivative with respect to thickness is

$$d^2E_{\text{cell}}/dt^2=[\nu/(2-\delta_{\nu,2})](d^2E_c/ds_e^2) \tag{7}$$

since s_i is constant for infinitesimal displacement of the surfaces. L_i' is then

$$L_i=[|2E_d|/(d^2E_{\text{cell}}/dt^2|_{\min})]^{1/2} . \tag{8}$$

For $\nu=2$ this expression reduces to the previously used value. For the limit $\nu\to\infty$ the expression becomes

$$L_i'(\infty)=[2|E_c(\infty)-E_c(1)|/(d^2E_c(\infty)/dc^2)]^{1/2} . \tag{9}$$

Table VI displays the calculated L_i' as a function of ν. Notice that the calculated infinite system limit for L_i' agrees decently with the completely independent L_s value from Ref. 32. Next note that although $L_i'(2)$ is almost exactly equal to L_s (probably fortuitously so), all the remaining values are much larger and decline with increasing ν. This vivid QSE should have consequences for the equation of state at $T=0$ K of these systems. Also evident is a feature already encountered: even at $\nu=5$ the film does not resemble the crystal.

TABLE VI. Scale lengths for the universal equation of state (see text) of the ν layers (a.u.).

ν	L_i'	L_a
1		1.66
2	1.97	1.89
3	3.30	2.42
4	3.10	2.07
5	2.40	1.62
∞	2.05	
solid[a]		1.14
surf-surf[b]	1.95	

[a]Reference 27.
[b]Reference 32.

As remarked already, the intraplanar force constants are quite stiff compared to the interplanar values for a given ν. Because of the small size of the cross derivatives, an excellent approximation for calculation of the a axis scale length is

$$L_a=[|E_{\text{bind}}|/(d^2E_{\text{tot}}/da^2|_{\min})]^{1/2} , \tag{10}$$

with $E_{\text{bind}}(\nu)$ defined as before (Boettger *et al*;[9] the expression was misprinted there but the proper expression was actually used) as

$$E_{\text{bind}}(\nu)=E_c(\nu)-E_i(\nu)/\nu , \tag{11}$$

that is, a *pro rata* portion to the interplanar binding energy is removed for each plane [of course $E_i(1)=0$]. The values of L_a, also tabulated in Table VI, display a very strong QSE in making a cycle from the 1-L value upward 45% and back down to virtually the starting value by $\nu=5$. The whole range is quite different from the bulk crystal value. Thus, even though the a parameter itself has settled nicely to the crystalline value by $\nu=5$, the intraplanar stress-strain relationship has not.

IV. KOHN-SHAM ONE-ELECTRON ENERGIES

The customary cautions about interpretation of KS eigenvalues as proper one-quasi-particle energies apply to all this section. With that caveat, we show the Kohn-Sham energy bands and densities of states (DOS) for all five ν layers in Figs. 1–6. The symmetry labels for the two-dimensional Brillouin zone follow the conventions given by Terzibaschian and Enderlein.[34] Comparison with the bulk bcc,[35,36] fcc,[29] and hcp (Ref. 27) energy bands produces no surprises when different symmetries, LDA models, etc. are kept in mind. Wimmer's 1-L results[37] (which were calculated at the experimentally determined lattice parameter for the crystal) are also consistent with the present ones.

Three basic band parameters, the work function Φ ($=-E_F$), the density of states at the Fermi level $N(E_F)$, and the occupied band width W, are summarized in Table VII. An optimistic interpretation of the ν dependence of Φ and $N(E_F)$ is that they are suggestive of the quantum size oscillations predicted from jellium mod-

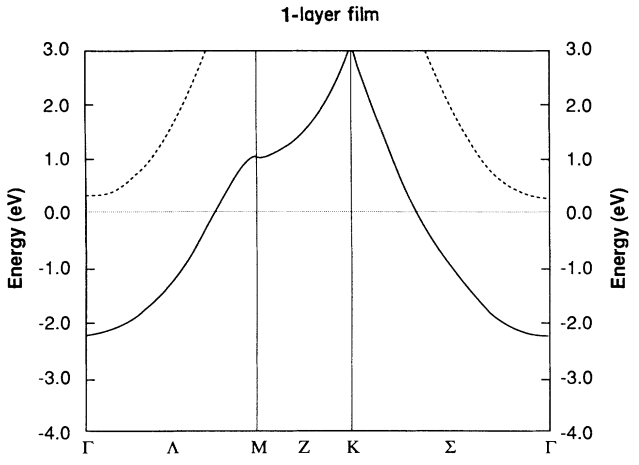

FIG. 1. Kohn-Sham energy bands for the Li 1 layer. Energies are given relative to the Fermi energy, in eV. Solid (dashed) curves are associated with states of even (odd) symmetry with respect to reflection in the x,y plane.

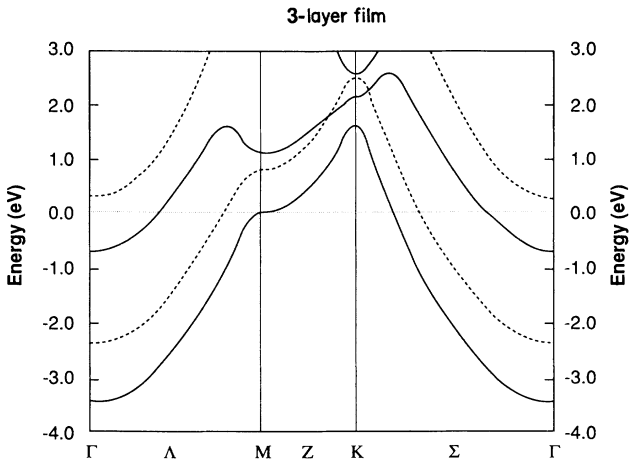

FIG. 3. Same as 1 but for the 3 layer.

els.[1,2] However, the amplitude of the nominal oscillation, 0.07 eV, is an order of magnitude smaller than that reported for unrelaxed Al films in Refs. 4 and 7.

In light of the technical limitations to determination of E_F (primarily proper representation of the large-z behavior of the charge density), we advance this interpretation cautiously. However, if the behavior of $\Phi(\nu)$ and $N(E_F,\nu)$ is a legitimate QSE, the unrelaxed lattice values of both quantities tabulated parenthetically in Table VII show clearly that lattice relaxation is critical to the prediction. Especially noteworthy is the behavior of $N(E_F)$ which differs qualitatively between equilibrium and unrelaxed cases. The equilibrium values exhibit a clear cycle in going through $\nu=1,\ldots,5$, while the unrelaxed values are, with the exception of $\nu=4$, essentially identical.

In Ref. 9, we had speculated that completion of the Li 3-L and 4-L calculations might be sufficient to allow a judgment as to the existence of QSE in Φ and $N(E_F)$ for ν layers of Li. That speculation now seems a trifle optimistic; knowledge of ν layers of Li through roughly $\nu=10$ may be required to reach a conclusion.

A *dramatic* quantum size effect does occur in the electronic density of states function $N(E)$ for the Li $\nu=1,\ldots,5$ sequence, in marked contrast to the situation with Φ and $N(E_F)$. To our knowledge it is essentially undiscussed in the literature, even though the underlying physics is quite straightforward. (Our previous study mentioned it almost as an afterthought.[9] Batra *et al.*[7] presented a somewhat related analysis which, however, obscures the central point for an alkali metal by use of a model 1-*d* potential).

For a system with two-dimensional periodicity, it is easy to show that a single parabolic band will produce a step-function density of states. This is the case with the Li 1 L. If addition of a layer perturbs that parabolic

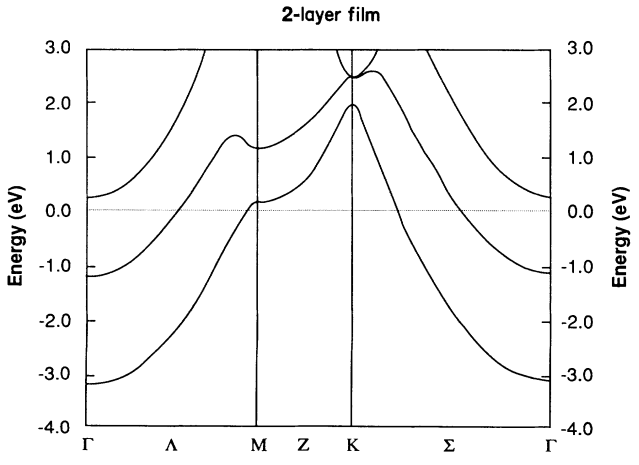

FIG. 2. Same as 1 but for the 2 layer and with no even-odd symmetry.

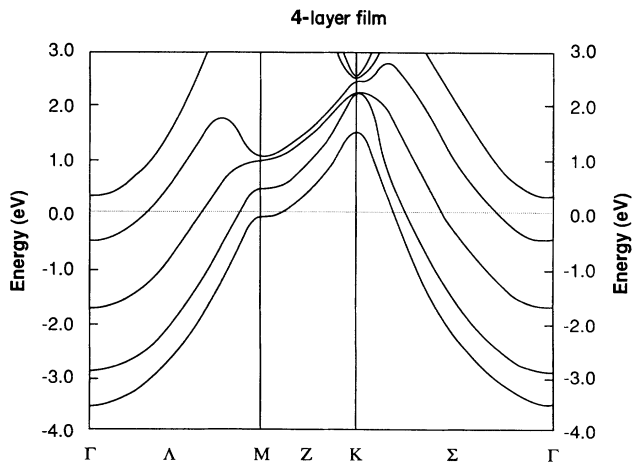

FIG. 4. Same as 2 but for the 4 layer.

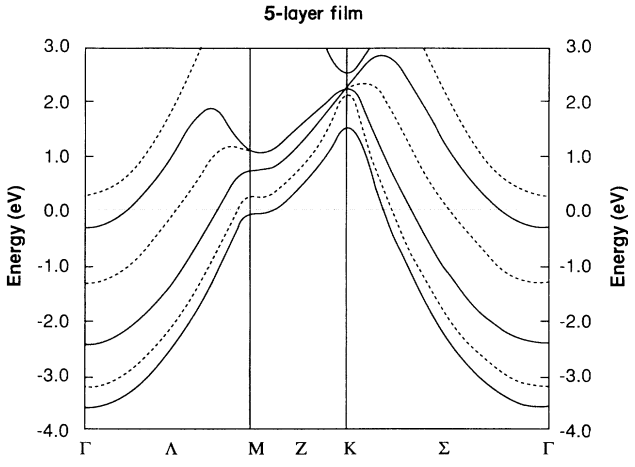

FIG. 5. Same as 1 but for the 5 layer.

band only weakly, as is the case with the ν layers of Li, then each integer increment in ν should generate an additional step in the DOS. Precisely such behavior is shown in the calculated densities of states displayed in Fig. 6. It is particularly striking that the strong lattice parameter differences between the films and the crystal do not combine to mask the effects predicted by the argument of weakly perturbed parabolic bands. As a result one has a directly testable prediction of strong one-electron QSE, namely an experimentally accessible qualitative feature which is in one-to-one correspondence with layer number.

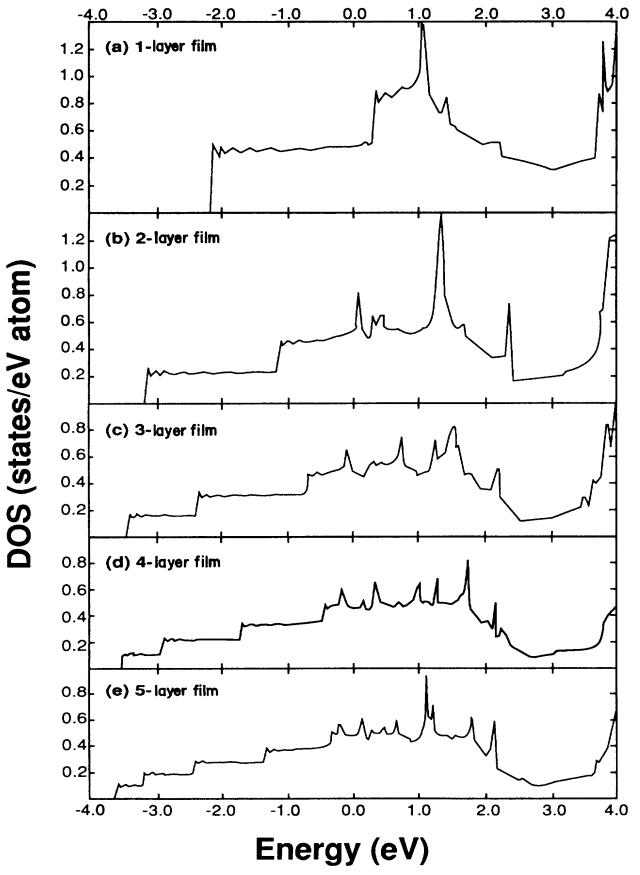

FIG. 6. The density of states (states/eV atom) as a function of one-electron energy (relative to the Fermi energy, eV) for the lithium films; (a) 1 layer; (b) 2 layer; (c) 3 layer; (d) 4 layer; (e) 5 layer.

TABLE VII. Calculated work function (Φ), density of states at the Fermi level [$N(E_F)$], and total occupied bandwidth (W) for the films, calculated crystalline data, and measured work function for the crystal. Parenthetical entries are for the film constrained to have calculated crystalline lattice parameters.

System	Φ (eV)	$N(E_F)$ (states/eV-atom)	W (eV)
1 L	3.56 (3.56)	0.49 (0.48)	2.2
2 L	3.63 (3.65)	0.55 (0.50)	3.1
3 L	3.60 (3.65)	0.58 (0.50)	3.4
4 L	3.61 (3.64)	0.46 (0.55)	3.5
5 L	3.56 (3.61)	0.47 (0.50)	3.6
crystal, bcc[a]		0.48	3.6
crystal, bcc[b]		0.49	3.8
crystal, expt.[c]	2.90		
1 L[d]	3.53	0.50	2.2
2 L[d]	3.58	0.56	3.2

[a]Reference 35.
[b]Reference 36.
[c]Reference 38.
[d]Reference 9.

We have previously remarked[9] on the systematic disparity between *all* calculated Li work-function values and the measured value.[38] The present calculations sustain the point: all modern calculations, irrespective of details of the model and method, give Φ about 0.5–0.6 eV larger than the measured value. In fact, the current value of the work function for the 1 L (3.56 eV) only differs from that obtained in Ref. 37 using the full-potential linear augmented plane wave method (3.53 eV) by 0.03 eV. Given the fact that the work function is the most sensitive quantity obtained in an LCGTO-FF calculation, this agreement clearly indicates the absence of any significant basis set effects in our 1-L results.

The previous 1- and 2-L study[9] found that the 2 L has essentially achieved its separated 1-L limit by an interplanar separation of about 12 a.u. That result led to the suggestion that the 5-L system might very well have its two surface layers effectively decoupled (since the 5-L thickness would be 17–18 a.u.). This suggestion is confirmed by the convergence of E_F, $N(E_F)$, and W to stable values by $\nu=5$. The latter two in particular agree well with theoretical crystalline values (cf. Table VI). The behavior of $N(E_F)$ is simply an indication that the interior electronic states of the 5 L are relatively bulklike. However, the fact that W has stabilized on the calculated crystalline value indicates that the surface-layer-to-surface-layer coupling is insignificant by $\nu=5$. In effect, by $\nu=5$ the system is simply filling in the projected bulk bands.

V. CONCLUSIONS

The Li 1, . . . , 5-L sequence is predicted to display strong QSE in the density of states and in the intraplanar force constants. Perhaps ironically, little or no QSE is to be expected in the conventional QSE quantity, the work function. Evidently this is a consequence of the fact that, except for its equilibrium band structure, relatively little about Li is free-electron-like. The primary feature of Li electronic states which tends to suppress work-function QSE is their dominant s-like character and associated low hybridization.

Several structural QSE manifestations are predicted: contracted interplanar separations, odd-even alteration of nearest-neighbor distances and outer layer interplanar separations, and an island (at $\nu=3$, 4, and 5) of stable s/a ratios reduced with respect to the bulk crystal value. The intraplanar stress-strain relationship (equation of state) is also predicted to exhibit strong QSE. For the 5 layer, the intraplanar lattice parameter a, $N(E_F)$, and W are all reasonably crystalline. Otherwise, little about these ν layers resembles the ideal crystal.

ACKNOWLEDGMENTS

This work was supported in part by the U.S. Department of Energy. S.B.T. also was supported in part by the U.S. Army Research Office. He thanks D. M. Parkin and A. M. Boring for arranging the visit in the Center for Materials Science, Los Alamos National Laboratory, during which part of this work was undertaken.

APPENDIX

For fitting $E_c(s)$, the cohesive energy as a function of a single structural parameter s, a least-squares fit to either a cubic function or to a functional form based on the so-called universal equation of state (see discussion and references above),

$$E_c(s)=C_1[1.0+C_2(s-s_0)]\exp[-C_2(s-s_0)]+C_3 , \tag{A1}$$

was used. The form that gave the smaller rms deviation was used. (Typically there was little to choose between them.) For fitting the simultaneous variation of E_c with respect to two structural parameters s, t it was convenient to use the generalized cubic form

$$E_c(s,t)=\sum_{n=0}^{3}\sum_{m=0}^{n} C_{mn}s^{(3-n)}t^{m} . \tag{A2}$$

Six evenly spaced 1-L values in the range $5.60\le a\le 5.85$ a.u. were sufficient to determine that the cubic fit and universal equation-of-state (EOS) fits were indistinguishable. For the 2 L, E_c values for 28 calculated points ($5.65\le a\le 5.85$, $s=3.86048$, 4.018 24, 4.176, 4.333 76, 4.482 24, 4.64 a.u.; for both $a=5.65$ and 5.75, $s=3.86048$ was unneeded) were fitted to the generalized cubic form.

Essentially the same procedure, but with only 24 points, was used for $\nu=3$. Twenty were on the grid $5.65\le a\le 5.85$, $s=4.176$, 4.333 76, 4.482 24, 4.64 a.u. The remaining four were $a=5.60$, 5.90 and $s=4.333\,76$, 4.482 24 a.u. This point distribution was driven by the need to explore and describe the rather long, shallow minimum as a function of a which seems to be peculiar to the 3 L.

For $\nu=4$ and 5 the first optimization was with respect to a sixteen-point s_i, s_e grid with a fixed at the calculated bulk value ($a=5.65$; $s_i,s_e=4.176$, 4.333 76, 4.482 24, 4.64 a.u.), followed by a generalized cubic fit. For $\nu=4$, the fitted s_i and s_e values (4.38 and 4.32 a.u., respectively) lay close enough to a mesh point (4.333 76, 4.333 76) that they could be fixed at those mesh values and a then varied over five equally spaced values ($5.60\le a\le 5.80$ a.u.). Both the cubic form and the universal EOS were fitted to the resulting calculated values. For the 5 L, essentially the same procedure was followed except that it was appropriate to fix s_i and s_e at the actual fitted values during the variation of a.

*Permanent address: Quantum Theory Project, Department of Physics and Department of Chemistry, University of Florida, Gainesville, FL 32611.

[1]F. K. Schulte, Surf. Sci. **55**, 427 (1976).
[2]E. E. Mola and J. L. Vicente, J. Chem. Phys. **84**, 2876 (1986).
[3]P. Feibelman, Phys. Rev. B **27**, 1991 (1983).
[4]P. Feibelman and D. R. Hamann, Phys. Rev. B **29**, 6463 (1984).
[5]K. M. Ho and K. P. Bohnen, Phys. Rev. B **29**, 3446 (1985).
[6]S. Ciraci and I. P. Batra, Phys. Rev. B **33**, 4294 (1986).
[7]I. P. Batra, S. Ciraci, G. P. Srivastava, J. S. Nelson, and C. Y. Feng, Phys. Rev. B **34**, 8246 (1986).
[8]J. L. Vicente, A. Paola, A. Razzitte, E. E. Mola, and S. B. Trickey, Phys. Status Solidi B **155**, K93 (1989).
[9]J. C. Boettger, S. B. Trickey, F. Müller-Plathe, and G. H. F. Diercksen, J. Phys. Condens. Matter **2**, 9589 (1990).
[10]J. C. Boettger and S. B. Trickey, J. Phys. F **14**, L151 (1984).
[11]J. C. Boettger and S. B. Trickey, Phys. Rev. B **32**, 1356 (1985).
[12]J. C. Boettger and S. B. Trickey, Phys. Rev. B **34**, 3604 (1986).
[13]J. Z. Wu, R. Sabin, S. B. Trickey, and J. C. Boettger, Int. J. Quantum Chem. Symp. **24**, 873 (1990).
[14]S. B. Trickey, G. H. F. Diercksen, and F. Müller-Plathe, Astrophys. J. **336**, 137 (1989).
[15]J. C. Boettger and S. B. Trickey, J. Phys. F **16**, 693 (1986).
[16]J. C. Boettger and S. B. Trickey, J. Phys. Condens. Matter **1**, 4323 (1989).
[17]E. S. Kryachko and E. V. Ludeña, *Energy Density Functional Theory of Many-Electron Systems* (Kluwer, Dordrecht, 1990).
[18]R. M. Dreizler and E. K. U. Gross, *Density Functional Theory* (Springer, Berlin, 1990).
[19]*Density Functional Theory of Many-Fermion Systems,* Vol. 21 of *Advances in Quantum Chemistry,* edited by S. B. Trickey (Academic, San Diego, 1990).

[20]J. W. Mintmire, J. R. Sabin, and S. B. Trickey, Phys. Rev. B **26**, 1743 (1982).
[21]F. B. van Duijneveldt (unpublished).
[22]T. H. Dunning and P. J. Hay, in *Methods of Electronic Structure Theory,* edited by H. F. Schaeffer (Plenum, New York, 1977), p. 1.
[23]B. I. Dunlap, J. W. D. Connolly, and J. R. Sabin, J. Chem. Phys. **71**, 3396 (1979).
[24]R. J. Gooding and J. A. Krumhansl, Phys. Rev. B **38**, 1695 (1988).
[25]M. M. Dacorogna and M. L. Cohen, Phys. Rev. B **34**, 4996 (1986).
[26]J. C. Boettger and R. C. Albers, Phys. Rev. B **39**, 3010 (1989).
[27]J. A. Nobel, S. B. Trickey, P. Blaha, and K. Schwarz (unpublished).
[28]H. J. F. Jansen, K. B. Hathaway, and A. J. Freeman, Phys. Rev. B **30**, 6177 (1984).
[29]J. C. Boettger and S. B. Trickey, Phys. Rev. B **32**, 3391 (1985).
[30]P. Blaha and K. Schwarz, J. Phys. F **17**, 899 (1987).
[31]C. S. Barrett, Acta Crystallogr. **9**, 671 (1956).
[32]J. H. Rose, J. R. Smith, and J. Ferrante, Phys. Rev. B **28**, 1835 (1983).
[33]P. Vinet, J. H. Rose, J. Ferrante, and J. R. Smith, J. Phys. Condens. Matter **1**, 1941 (1989).
[34]T. Terzibaschian and R. Enderlein, Phys. Status Solidi B **133**, 443 (1986).
[35]V. L. Moruzzi, J. F. Janak, and A. R. Williams, *Calculated Electronic Properties of Metals* (Pergamon, New York, 1978).
[36]D. A. Papaconstantopoulos, *Handbook of Band Structures of Elemental Solids* (Plenum, New York, 1986).
[37]E. Wimmer, J. Phys. F **13**, 2313 (1983).
[38]H. B. Michaelson, J. Appl. Phys. **48**, 4729 (1977).